The Cu-Gd (Copper-Gadolinium) System

By P.R. Subramanian and D.E. Laughlin
Carnegie Mellon University

Equilibrium Diagram

The equilibrium phases of the Cu-Gd system are: (1) the liquid, L, without any miscibility gaps; (2) the fcc terminal solid solution, (Cu), with negligible solid solubility of Gd in (Cu); (3) the Gd-rich bcc terminal solid solution, (βGd), based on the equilibrium phase of pure Gd between 1235 and 1313 °C; (4) the Gd-rich cph terminal solid solution, (αGd), stable below 1235 °C; (5) the hexagonal intermediate phase, Cu_7Gd, stable only at elevated temperatures; (6) the orthorhombic intermediate phase, Cu_6Gd, stable up to the peritectic melting temperature of 865 °C; (7) Cu_5Gd, present in two allotropic modifications (the lower temperature cubic form is stable up to 870 °C and the high-temperature hexagonal form is stable between 870 °C and the peritectic melting temperature of 925 °C); (8) Cu_9Gd_2, with an unknown crystal structure, and stable up to the congruent melting temperature of 930 °C; (9) Cu_7Gd_2, with an unknown crystal structure and stable between 825 and 870 °C; (10) the orthorhombic phase, Cu_2Gd, stable up to the congruent melting temperature of 860 °C; and (11) the most Gd-rich intermediate phase, CuGd, with a cubic structure, stable up to the congruent melting temperature of 830 °C.

The earliest Cu-Gd phase diagram investigation was by [64Cop], who proposed the occurrence of a eutectic reaction between (αGd) and CuGd at ~70 at.% Gd. The investigation of [64Cop] was partial and restricted to the region between 50 to 100 at.% Gd. Subsequently, [83Car] and [83Che] independently determined the Cu-Gd phase diagram by means of differential thermal analysis (DTA), X-ray diffraction, and metallography. The two reports agree with regard to the existence of Cu_6Gd, Cu_5Gd, Cu_2Gd, and CuGd. In addition, melting points reported for Cu_6Gd, Cu_5Gd, and Cu_2Gd by [83Car] and [83Che] agree. However, [83Car] reported the peritectic formation of Cu_5Gd and the congruent formation of Cu_9Gd_2, Cu_2Gd, and CuGd, whereas [83Che] reported the congruent formation of Cu_5Gd and the peritectic formation of Cu_2Gd and CuGd. Moreover, [83Che] did not report the existence of a phase with the stoichiometry Cu_9Gd_2. Similar discrepancies are observed in the Cu-Dy system. The basic features of the Cu-Gd phase diagram of [83Che] essentially are in agreement with those of the Cu-Dy system reported by the same group [82Che]. Similarly, the Cu-Gd phase diagram of [83Car] closely resembles the Cu-Dy phase diagram of [82Fra]. In addition, the general features of the Cu-Gd phase diagram of [83Car] are in good accord with those of Cu-Er [70Bus1] and those of Cu-Y [81Cha]. The alloying behavior of Cu with the heavy lanthanides is expected to be systematic as one proceeds down the lanthanide series, and the alloying behavior of Y parallels that of the heavy lanthanides [85Gsc]. In this respect, the Cu-Gd phase diagram of [83Car] closely follows the systematics of Cu with the heavy lanthanides.

Fig. 1 Assessed Cu-Gd Phase Diagram

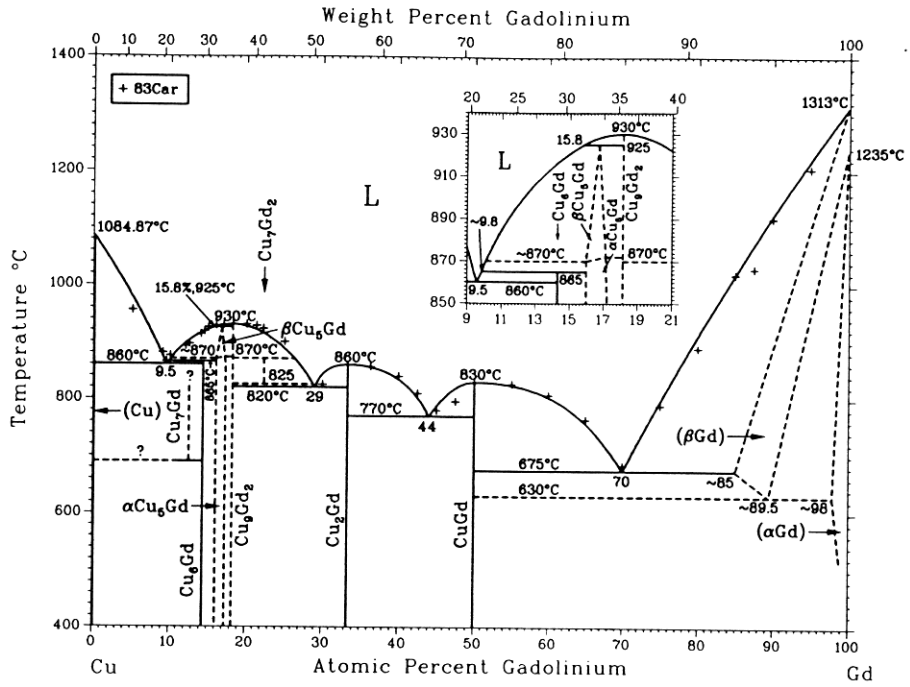

P.R. Subramanian and D.E. Laughlin, 1988.

Table 1 Cu-Gd Experimental Liquidus Data

Composition, at.% Gd	Temperature, °C	Composition, at.% Gd	Temperature, °C
5.0	955	33.3	860
9.0	880	36.3	857
9.5	865	40.0	840
10	875	42.5	810
12.0	892	45.0	780
12.5	896	47.5	796
14.0	913	50.0	830
14.5	918	55.0	827
15.0	925	60.0	808
16.0	928	65.0	765
17.0	929	70.0	684
18.2	930	75.0	790
20.0	930	80.0	890
21.3	928	85.0	1020
22.2	923	87.5	1030
25.0	900	90.0	1118
30.0	825	95.0	1205

From [83Car].

The assessed Cu-Gd equilibrium diagram is shown in Fig. 1. The diagram is based on the report of [83Car], with adjustments in the elemental melting points in accordance with the accepted values listed in [Melt] for Cu and [78Bea] and [86Gsc] for (βGd). The (αGd) ↔ (βGd) transformation temperature has been changed from 1265 to 1235 °C to bring it into agreement with the accepted value given in [78Bea] and [86Gsc]. Minor changes have also been made in the liquidus in the vicinity of the congruent point at 830 °C to conform to thermodynamic rules for construction of congruent inflection points [81Goo], and consequently, the eutectic composition at 770 °C has been slightly shifted toward higher Gd content.

Terminal Solid Solubility

There is no evidence of any terminal solid solubility of Gd in Cu. [64Cop] estimated the terminal solid solubility of Cu in (αGd) to be less than 0.5 at.%. On the other hand, [83Car] reported that (αGd) has a maximum solid solubility of ~2 at.% Cu at 630 °C. The phase diagram reported by [83Car] in the Gd-rich end, shown in Fig. 2, is quite unusual in that (βGd) is reported to have a maximum solid solubility of ~15 at.% Cu at the eutectic temperature of 675 °C, and (βGd) is shown to decompose to (αGd) and CuGd through a eutectoid reaction at 89.5 at.% Gd and 630 °C. There are no solvus data to support the large homogeneity range of (βGd), although the eutectoid temperature of 630 °C has been derived from DTA on alloys containing 55 to 98 at.% Gd. Such behavior in the lanthanide-rich end has not been reported for any of the other Cu-heavy lanthanide systems; however, it has been found in the Cu-Ce system [64Rhi] (see also Cu-Ce, in this issue). The eutectoid reaction, as well as the accompanying phase relationships in the Gd-rich

Fig. 2 Cu-Gd Phase Diagram of [83Car] in the Gd-Rich Region

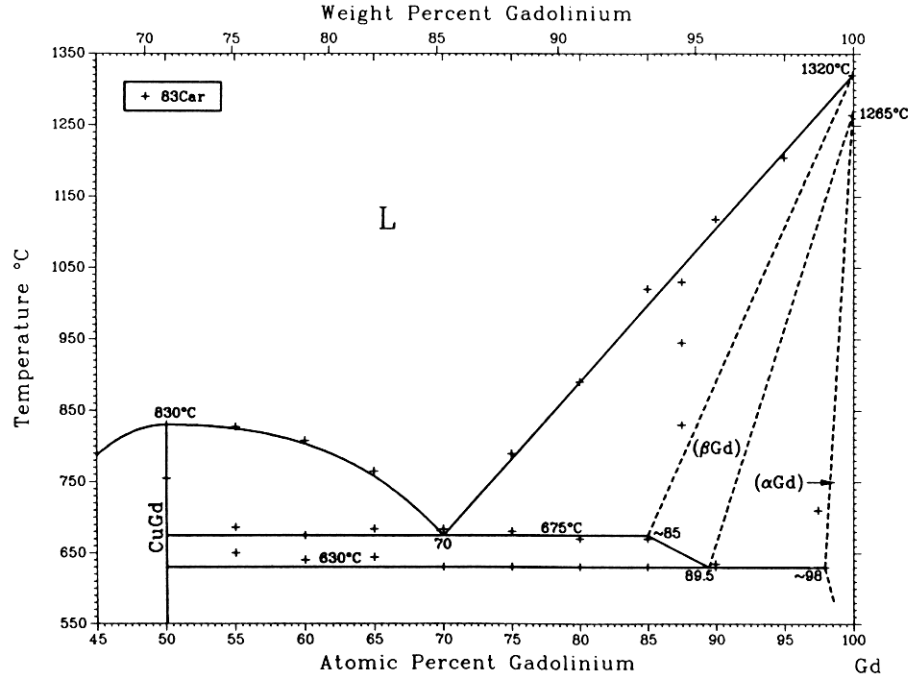

Melting and transformation temperatures are in error; see Fig. 1 for accepted values.

P.R. Subramanian and D.E. Laughlin, 1988.

end, are shown as dashed lines in the assessed phase diagram in Fig. 1. Further work needs to be done at the Gd-rich end to determine the exact nature of the (αGd) ↔ (βGd) transformation.

Liquidus and Solidus

Experimental data for the Cu-Gd liquidus boundaries are shown in Table 1. The melting points of (Cu) and (βGd) are accepted as 1084.87 °C [Melt] and 1313 °C [78Bea, 86Gsc], respectively.

Table 2 summarizes the various invariant reactions observed for the Cu-Gd system. Four eutectic reactions were observed: Cu-Cu_6Gd (860 °C, 9.5 at.% Gd); Cu_9Gd_2-Cu_2Gd (820 °C, 29 at.% Gd); Cu_2Gd-CuGd (770 °C, 44.0 at.% Gd); and CuGd-Gd (675 °C, 70 at.% Gd). In all the reactions, the eutectic temperatures reported by [83Car] are in good agreement with the systematics observed for the corresponding eutectic temperatures in the other Cu-lanthanide systems (see "The Copper-Rare Earth Systems," in this issue). [83Car] observed an unusual thermal effect at 755 °C in alloys containing 36.5 to 50 at.% Gd. Because Cu_2Gd and CuGd do not show any transformations near 755 °C, the present evaluators are unable to find any specific explanations for this effect.

Intermediate Phases

There is a conflict with regard to the stoichiometry of the phase in equilibrium with the (Cu) terminal solution. [71Bus] reported the high-temperature formation of Cu_7Gd, with its subsequent decomposition to Cu_6Gd and (Cu) upon annealing at temperatures below 700 °C. In addition, [71Bus] prepared a sample corresponding to the composition $Cu_{6.5}Gd$ and subjected it to an annealing treatment at 700 °C for three weeks, followed by quenching. Metallographic and X-ray examination showed that the quenched sample of $Cu_{6.5}Gd$ contained a two-phase mixture of Cu_7Gd and Cu_6Gd in appropriate amounts, with the lattice parameters of Cu_7Gd in the two-phase region corresponding to those obtained for Cu_7Gd in the single-phase condition. On the other hand, [83Car] found no evidence of this phase in their thermal and metallographic analyses. Their phase diagram shows the most Cu-rich phase to be Cu_6Gd, forming peritectically at 865 °C from the liquid and Cu_5Gd. However, [83Car] did not rule out the existence of Cu_7Gd completely, because X-ray examination of samples with a Cu content near that of Cu_7Gd revealed the existence of a phase with a structure closely related to the $CaCu_5$ type, with lattice parameters between that of the 1-to-

Table 2 Special Points of the Assessed Cu-Gd Phase Diagram

Reaction	Compositions of the respective phases, at.% Gd			Temperature, °C	Reaction type	Reference
(Cu) ↔ L		0.0		1084.87	Melting point	[Melt]
L ↔ (Cu) + Cu_6Gd	9.5	~0	14.29	860	Eutectic	[83Car]
L + Cu_5Gd ↔ Cu_6Gd	~9.8	~16	14.29	865	Peritectic	[83Car](a)
L + Cu_9Gd_2 ↔ Cu_5Gd	~15.8	18.18	16.67	925	Peritectic	[83Car](a)
L ↔ Cu_9Gd_2		18.18		930	Congruent	[83Car]
L ↔ Cu_9Gd_2 + Cu_2Gd	29.0	18.18	33.33	820	Eutectic	[83Car]
L ↔ Cu_2Gd		33.33		860	Congruent	[83Car]
L ↔ Cu_2Gd + CuGd	~44	33.3	50.0	770	Eutectic	[83Car](a)
L ↔ CuGd		50.0		830	Congruent	[83Car]
L ↔ CuGd + (αGd)	70.0	50.0	~85.0	675	Eutectic	[83Car]
(βGd) ↔ CuGd + (γGd)	~89.5	50.0	~98.0	630	Eutectoid	[83Car]
(αGd) ↔ (βGd)		~100		1235	Allotropic	[78Bea, 86Gsc]
(βGd) ↔ L		100		1313	Melting point	[78Bea, 86Gsc]

(a) Liquidus composition was obtained by interpolation of experimental data in Fig. 1.

5 phase and that of the 1-to-7 phase reported by [71Bus]. [83Che] examined alloys with compositions between those of (Cu) and Cu_6Gd by thermal analysis and X-ray diffraction and failed to observe Cu_7Gd. [71Bus] have not reported the temperature of formation of Cu_7Gd. Examination of the assessed phase diagram in Fig. 1 shows that Cu_7Gd can form either peritectically from the liquid and Cu_6Gd at a temperature between the eutectic invariant (860 °C) and the peritectic invariant (865 °C), or peritectoidally from (Cu) and Cu_6Gd at a temperature below the eutectic invariant. In view of the narrow temperature range between the eutectic and peritectic invariants, the former reaction is ruled out, and therefore it is quite likely that Cu_7Gd forms through the latter reaction, with subsequent decomposition below 700 °C through a eutectoid reaction.

Cu_5Gd is observed to exist in two allotropic modifications, (αCu_5Gd) and (βCu_5Gd), with [83Car] reporting a large homogeneity range in both the allotropic forms. The high-temperature form, (βCu_5Gd), decomposes peritectically at 925 °C, and undergoes a transformation to the (αCu_5Gd) modification at ~660 °C. This polymorphic transition temperature is probably too low; systematics of Cu-lanthanide systems suggests a value of ~870 °C for the α ↔ β transition temperature. [71Bus] reported that the hexagonal (βCu_5Gd) modification is metastable and could be obtained in the single-phase condition only in splat-cooled alloys, implying that the cubic ($\alpha Cu5Gd$) form is the stable phase at all temperatures below the peritectic invariant.

[83Car] reported the formation of a phase at ~18.2 at.% Cu and assigned it a stoichiometry of Cu_9Gd_2 on the basis of thermal analysis and metallography. Cu_9Gd_2 is reported to melt congruently at 930 °C. Another phase with the stoichiometry Cu_7Gd_2 was detected by [83Car] at ~22.3 at.% Cu on the basis of thermal effects only. This phase was found to exist with a limited temperature range of stability and formed peritectically at 870 °C, with subsequent decomposition at 825 °C.

[83Car] reported that Cu_2Gd and CuGd melt congruently at 860 and 830 °C, respectively. In contrast, the diagram of [83Che] shows both Cu_2Gd and CuGd melting peritectically at 870 and 759 °C, respectively. However, the corresponding 2-to-1 and 1-to-1 phases in the Cu-Y [81Cha], Cu-Dy [82Fra], and Cu-Er [70Bus1] systems all melt congruently. Alloys of Cu with the heavy lanthanides, as well as Y, are expected to show a systematic trend with regard to melting behavior. In this respect, the data reported by [83Car] are consistent with the systematics, and therefore are accepted in Fig. 1.

Metastable Phases

[72Ray] obtained metastable solid solutions of Cu in Gd with up to 10 to 12.5 at.% Cu under conditions of splat cooling. Mössbauer studies of the quenched samples indicated the complete absence of equilibrium intermediate phases in the resultant solid solutions.

[74Dom] prepared thin-film samples of Cu_2Gd by thermal evaporation, followed by condensation under vacuum onto glass substrates preheated to 200 °C. The resultant thin-film specimens were 100 to 150 nm thick and could be indexed by X-ray diffraction on the basis of the $MgCu_2$ (Laves phase) type unit cell with a = 0.750 nm.

[79Mcg] obtained amorphous films with the stoichiometry $Cu_{0.58}Gd_{0.42}$ by sputtering from arc-melted specimens and by thermal evaporation, followed by deposition on liquid nitrogen-cooled sapphire substrates. The thin films produced in this manner were 500 to 1000 nm thick and were characterized by

Table 3 Cu-Gd Experimental Lattice Parameters

Phase	Crystal structure	Lattice parameters, nm a	b	c	Reference
Cu_7Gd	Hexagonal	0.4951	...	0.4171	[71Bus](a)
Cu_6Gd	Orthorhombic	0.8040	0.5009	0.9995	[70Bus2]
		0.8035	0.5019	1.0010	[83Car]
Cu_5Gd	Hexagonal	0.5018	...	0.4117	[59Wer]
		0.5039	...	0.4111	[71Bus](b)
		0.5036	...	0.4102	[83Car](c)
Cu_5Gd	Cubic	0.706	...	...	[69Bus](d)
Cu_9Gd_2	(e)	0.500	...	1.39	[83Car]
Cu_2Gd	Orthorhombic	0.4320	0.6858	0.7330	[62Sto]
		0.4333	0.6888	0.7375	[82Gra]
		0.4328	0.6878	0.7343	[83Car]
CuGd	Cubic	0.3505	...	...	[61Gsc]
		0.3503	...	...	[61Bae]
		0.3502	...	...	[65Gsc, 83Don]
		0.3501	...	...	(f)

(a) Reported to be stable only at high temperatures. (b) Observed only in splat-cooled samples. (c) High-temperature modification; reported to be stable between 660 and 925 °C. (d) Could not be obtained as a single phase; contained small amounts of the hexagonal modification. (e) Structure based on a tetragonal cell. (f) [66Sek, 72Bur, 80Gef, 83Car].

Table 4 Cu-Gd Crystal Structure Data

Phase	Composition, at.% Gd	Pearson symbol	Space group	Strukturbericht designation	Prototype
(Cu)	0	$cF4$	$Fm\bar{3}m$	$A1$	Cu
Cu_6Gd	~14.29	$oP28$	$Pnma$	...	$CeCu_6$
Cu_5Gd(HT)	~16 to ~17.3	$hP6$	$P6/mmm$	$D2_d$	$CaCu_5$
Cu_5Gd(LT)	~16 to ~17.3	$cF24$	$F\bar{4}3m$	$C15_b$	$AuBe_5$
Cu_2Gd	~33.3	$oI12$	$Imma$	...	$CeCu_2$
CuGd	~50	$cP2$	$Pm\bar{3}m$	$B2$	CsCl
(αGd)	~98.2 to 100	$hP2$	$P6_3/mmc$	$A3$	Mg
(βGd)	~100	$cI2$	$Im\bar{3}m$	$A2$	W

electron microprobe analysis to give the sample stoichiometry.

Crystal Structures and Lattice Parameters

Table 3 lists the experimental values for the lattice parameters of the various Cu-Gd intermediate phases. The accepted lattice parameter data, crystal structures, and related parameters for the various phases are shown in Tables 4 and 5.

According to [71Bus], Cu_7Gd forms with a hexagonal crystal structure related to that of the $CaCu_5$ type with lattice parameters a = 0.4951 nm, and c = 0.4171 nm and with the space group $P6/mmm$. From experimental X-ray data on Cu_7Tb, [71Bus] concluded that the actual stoichiometry for the 7-to-1 phases is $Cu_{5.44}RE_{0.78}$ (RE = Gd, Tb, Dy, and Y) with 22% of the RE sites substituted at random by pairs of Cu atoms.

From X-ray diffraction measurements, [70Bus2] determined that Cu_6Gd forms with the orthorhombic $CeCu_6$ structure. Lattice parameters reported for this phase by [70Bus2] and [83Car] are in good agreement.

The report of [83Car] shows that Cu_5Gd is dimorphic, with the high-temperature form crystallizing with the hexagonal $CaCu_5$-type structure and the low-temperature form crystallizing with the cubic $AuBe_5$-type structure. [71Bus] reported that the hexagonal form of Cu_5Gd was obtained as single phase only under rapid cooling. Lattice parameters reported for the hexagonal Cu_5Gd by [59Wer], [71Bus], and [83Car] show slight variations from one another that can arise as a result of the large homogeneity field observed for Cu_5Gd by [83Car]. The data of [83Car] have been obtained from samples of stoichiometric composition and with higher purity starting materials, and therefore, have been accepted in Table 5. [83Car] have not determined the lattice constant of the low-temperature cubic modification of Cu_5Gd. [69Bus] have reported the occurrence of a fcc structure with lattice parameter a = 0.706 nm in both as-cast and annealed alloys with the composition Cu_5Gd. However, these alloys were not obtained as single phases, and even after annealing, they contained small amounts of the high-temperature hexagonal phase.

Preliminary X-ray measurements by [83Car] indicated that Cu_9Gd_2 has a tetragonal symmetry with a

Fig. 3 Assessed vs Calculated Cu-Gd Phase Diagram

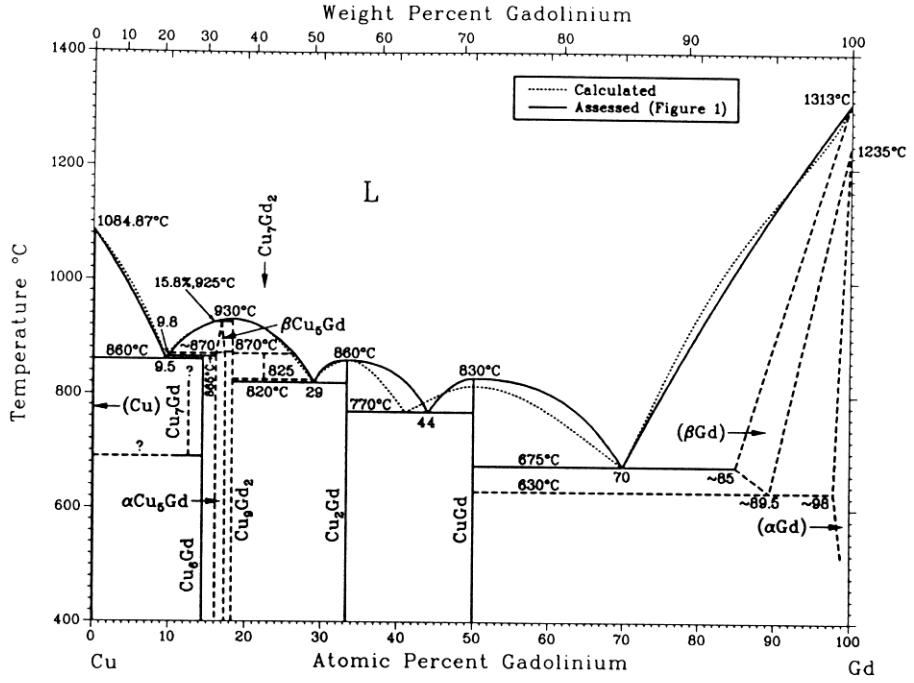

P.R. Subramanian and D.E. Laughlin, 1988.

Table 5 Cu-Gd Lattice Parameter Data

Phase	Composition, at.% Gd	Lattice parameters, nm a	b	c	Comment	References
(Cu)	0	0.36146	...	...	At 25 °C	[Massalski]
Cu_6Gd	~14.29	0.8038	0.5014	1.0003	...	[70Bus2, 83Car]
Cu_5Gd(HT)	~16 to ~17.3	0.5036	...	0.4102	(a)	[83Car]
Cu_5Gd(LT)	~16 to ~17.3	0.706	...	...	(b)	[69Bus]
Cu_2Gd	~33.3	0.4327	0.6875	0.7349	...	(c)
CuGd	~50	0.3502	...	...	...	(d)
(αGd)	~98.2 to 100	0.36336	...	0.57810	At 24 °C	[78Bea, 86Gsc]
(βGd)	~100	0.406	...	...	At 1265 °C	[78Bea, 86Gsc]

(a) Stable between 870 and 925 °C. (b) Low-temperature modification; sample contained small amounts of the high-temperature hexagonal phase. (c) [63Sto, 82Gra, 83Car]. (d) [61Bae, 65Gas, 66Sek, 72Bur, 80Gef, 83Don, 83Car].

= 0.5 nm and c = 1.39 nm (minimum). Although no structural details were obtained by [83Car], the powder patterns for Cu_9Gd_2 were observed to be similar to those of Cu_9Dy_2 [82Fra] and Cu_9Yb_2 [71Ian].

Cu_2Gd crystallizes with the orthorhombic $CeCu_2$ structure, and the accepted lattice parameters in Table 5 are based on the data of [63Sto], [82Gra], and [83Car].

The equiatomic phase, CuGd, forms with the cubic CsCl structure, and the lattice parameters reported by various researchers are in good agreement. [68Wij] reported the tendency for CuGd to undergo a structural transformation from the cubic CsCl structure to the orthorhombic FeB structure at ~75 K, based on magnetic susceptibility measurements. Subsequently, [83Don] reported that their electrical resistivity, magnetic susceptibility, thermal expansion, X-ray diffraction, and differential scanning calorimetry (DSC) measurements show evidence of a partial transformation to the low-temperature FeB structure at ~250 K. Moreover, [83Don] stated that this transformation is associated with large hysteresis effects, with the reverse transformation into the CsCl structure occurring at ~600 K. Earlier, [80Gef] and [81Gef] had noticed a similar hysteresis in their elastic constant, electrical resistivity, and dilatometric measurements, but could not corroborate this by X-ray diffraction or metallography.

Table 6 Cu-Gd Thermodynamic Properties

Lattice stability parameters for Cu(a)

$G^0(Cu, L) = 0$

$G^0(Cu, fcc) = -13\,054 + 9.613\,T$

Lattice stability parameters for Gd(b)

$G^0(Gd, L) = 0$

$G^0(Gd, bcc) = -10\,050 + 6.336\,T$

$G^0(Gd, cph) = -13\,960 + 8.929\,T$

Integral molar Gibbs energies(c)

$G(L) = X(1-X)(-96\,712 + 47\,780\,X) + RT[X \ln X + (1-X) \ln (1-X)]$

$\Delta_f G(Cu_6Gd) = -30\,147 + 13.12\,T$

$\Delta_f G(Cu_5Gd) = -27\,571 + 8.97\,T$

$\Delta_f G(Cu_9Gd_2) = -29\,257 + 9.49\,T$

$\Delta_f G(Cu_2Gd) = -25\,577 + 1.45\,T$

$\Delta_f G(CuGd) = -38\,873 + 13.25\,T$

Note: Standard states: pure liquid Cu and pure liquid Gd. Gibbs energies are expressed in J/mol, and temperatures are in K. X is the atomic fraction of Gd. Mol refers to the atom as the elementary entity.
(a) From [Hultgren,E] (b) From [83Cha]; melting and transformation temperatures are from [78Bea] and [86Gsc]. (c) From the phase diagram [this work].

Thermodynamics

There have been no reports on the thermodynamic properties of the Cu-Gd system. In the present modeling, the Gibbs energy of mixing for the liquid was estimated from the experimental liquidus data at the two eutectic points (9.5 at.% Gd, 860 °C and 70 at.% Gd, 675 °C). The following assumptions were made in the calculation: (1) terminal solid solubilities are negligible (the large solubility range for (βGd) was also neglected in the calculations); (2) the lattice stability parameters for Cu, bcc Gd, and cph Gd are as listed in Table 6; and (3) the liquid behaves like a subregular solution. The Gibbs energies of formation of Cu_6Gd, Cu_5Gd, Cu_9Gd_2, Cu_2Gd, and CuGd were then derived from the various liquidus temperatures, as well as the Gibbs energy of mixing for the liquid. In all instances, the phases have been treated as line compounds. Table 6 shows the values of the various parameters.

Liquidus temperatures were next evaluated across the phase diagram from the Gibbs energy functions listed in Table 6. The calculated phase boundaries (Fig. 3) are in good agreement with the experimental data, except for the region between Cu_2Gd and CuGd. The calculated eutectic composition at 770 °C is ~3 at.% lower in Gd content, as compared to the experimental composition. This discrepancy could be attributed to the simplicity of the present model, which always gives a symmetrical liquidus about an intermediate phase with nil homogeneity range. Barring this deficiency, the Gibbs energy functions listed in Table 6 reproduce the experimental phase boundaries with a reasonable degree of accuracy.

Table 7 Calculated Enthalpies of Formation of Cu-Gd Intermediate Phases vs Theoretical Estimates Based on Miedema's Model

Phase	Enthalpy of formation, kJ/mol: Present modeling	Miedema model(a)
Cu_6Gd	−30.2	−29.4
Cu_9Gd_2	−27.6	−32.0
Cu_4Gd	−29.3	−35.5
Cu_2Gd	−25.6	−45.3
CuGd	−38.9	−45.3

Note: Standard states are liquid Cu and liquid Gd.
(a) From [83Nie].

The enthalpies of formation from the present thermodynamic analysis are compared in Table 7 with those evaluated with the semi-empirical model of Miedema [80Mie, 83Nie]. The two results are closely comparable, with the exception of Cu_2Gd, for which the two estimates differ by almost 19 kJ/mol.

Cited References

59Wer: J.H. Wernick and S. Geller, "Transition Element-Rare Earth Compounds with the $CaCu_5$ Structure," *Acta Crystallogr., 12,* 662-665 (1959). (Crys Structure; Experimental)

61Bae: N.C. Baenziger and J.L. Moriarty, Jr., "Gadolinium and Dysprosium Intermetallic Phases. II. Laves Phases and Other Structure Types," *Acta Crystallogr., 14,* 948-950 (1961). (Crys Structure; Experimental)

61Gsc: K.A. Gschneidner, Jr., *Rare Earth Alloys,* D. Van Nostrand Co., Inc., Princeton, NJ, 154 (1961). (Crys Structure; Compilation)

63Sto: A.R. Storm and K.E. Benson, "Lanthanide-Copper Intermetallic Compounds having the $CeCu_2$ and AlB_2 Structure," *Acta Crystallogr., 16,* 701-702 (1963). (Crys Structure; Experimental)

64Cop: M. Copeland and H. Kato, "Rare-Earth-Rich Alloys," *Physics and Materials Problems of Reactor Control Rods,* International Atomic Energy Agency, Vienna, Austria, 295-317 (1964); also see Report No. USBM-U-1031, Quarterly Metallurgical Progress Report No. 18, U.S. Bureau of Mines, Albany Metallurgy Research Center, Albany, OR, 3-16 (1963). (Equi Diagram; Experimental; #)

64Rhi: T.B. Rhinehammer, D.E. Etter, J.E. Selle, and P.A. Tucker, "The Cerium-Copper System," *Trans. Met. Soc. AIME, 230,* 1193-1198 (1964). (Equi Diagram, Crys Structure; Experimental)

65Gsc: K.A. Gschneidner, Jr., "Crystal Structures of Some Equiatomic Gadolinium Compounds," *Acta Crystallogr., 18,* 1082-1083 (1965). (Crys Structure; Experimental)

66Sek: K. Sekizawa and K. Yasukochi, "Magnetic Properties of Rare Earth Intermetallic Compounds in Gd(Ag, Cd, In) and Gd(Cu, Ag, Au) Systems," *J. Phys. Soc. Jpn., 21*(4), 684-692 (1966). (Crys Structure; Experimental)

68Wij: H.W. de Wijn, K.H.J. Buschow, and A.M. van Diepen, "Experimental Evidence for Interband Mixing in Rare-Earth Intermediate Compounds," *Phys. Status Solidi, 30,*

759-766 (1968). (Crys Structure; Experimental)

69Bus: K.H.J. Buschow, A.S. van der Goot, and J. Birkhan, "Rare-Earth Copper Compounds with $AuBe_5$ Structure," *J. Less-Common Met., 19,* 433-436 (1969). (Crys Structure; Experimental)

70Bus1: K.H.J. Buschow, "The Erbium-Copper System," *Philips J. Res., 25,* 227-230 (1970). (Equi Diagram, Crys Structure; Experimental)

70Bus2: K.H.J. Buschow and A.S. van der Goot, "The Crystal Structure of Some Copper Compounds of the Type RCu_6," *J. Less-Common Met., 20,* 309-313 (1970). (Crys Structure; Experimental)

71Bus: K.H.J. Buschow and A.S. van der Goot, "Composition and Crystal Structure of Hexagonal Cu-Rich Rare Earth-Copper Compounds," *Acta Crystallogr. B, 27*(6), 1085-1088 (1971). (Crys Structure; Experimental)

71Ian: A. Iandelli and A. Palenzona, "The Ytterbium-Copper System," *J. Less-Common Met., 25,* 333-335 (1971). (Equi Diagram, Crys Structure; Experimental)

72Bur: E. Burzo, I. Urzu, and J. Pierre, "Electronic Spin Resonance and Magnetic Susceptibility of the Compounds GdCu and GdAg," *Phys. Status Solidi. (b), 51,* 463-467 (1972). (Crys Structure; Experimental)

72Ray: R. Ray, M. Segnini, and B.C. Giessen, "Concentrated Di-Substitutional Solid Solutions," *Solid State Commun., 10,* 163-167 (1972). (Meta Phases; Experimental)

74Dom: V.A. Domyshev, V.A. Yegorov, V.A. Buravikhin, L.M. Sidorenko, and N.I. Luzgin, "Crystalline Structure, Magnetic and Magnetoelastic Properties of Films of GdM_2 Compounds of the Laves Phase Type," *Fiz. Met. Metalloved., 38*(1), 102-109 (1974) in Russian; TR: *Phys. Met. Metall., 38*(1), 89-95 (1974). (Meta Phases; Experimental)

78Bea: B.J. Beaudry and K.A. Gschneidner, Jr., "Preparation and Basic Properties of the Rare-Earth Metals," in *Handbook on the Physics and Chemistry of Rare Earths,* Vol. 1-*Metals,* K.A. Gschneidner, Jr. and L. Eyring, Ed., North-Holland Physics Publishing Co., Amsterdam, 173-232 (1978). (Equi Diagram; Compilation)

79Mcg: T.R. McGuire and R.J. Gambino, "Magnetic and Transport Properties of Rare-Earth Au and Cu Amorphous Alloys," *J. Appl. Phys., 50*(11), 7653-7655 (1979). (Meta Phases; Experimental)

80Gef: Y. Gefen and M. Rosen, "On the Nature of the Hysteretic Behavior in GdCu Compounds," *Scr. Metall., 14,* 645-648 (1980). (Crys Structure; Experimental)

80Mie: A.R. Miedema, P.F. de Chatel, and F.R. de Boer, "Cohesion in Alloys - Fundamentals of a Semi-Empirical Method," *Physica B, 100,* 1-28 (1980). (Thermo; Theory)

81Cha: D.J. Chakrabarti and D.E. Laughlin, "The Copper-Yttrium System," *Bull. Alloy Phase Diagrams, 2*(3), 315-319 (1981). (Equi Diagram, Crys Structure; Review)

81Gef: Y. Gefen and M. Rosen, "Anomalous Elasticity and Anelasticity of GdCu at Low Temperatures," *J. Phys. Chem. Solids, 42*(9), 857-860 (1981). (Crys Structure; Experimental)

81Goo: D.A. Goodman, J.W. Cahn, and L.H. Bennett, "The Centennial of the Gibbs-Konovalov Rule for Congruent Points - Its Underlying Theoretical Basis and Its Application to Phase Diagram Evaluation," *Bull. Alloy Phase Diagrams, 2*(1), 29-34 (1981). (Thermo; Review)

82Che: C.S. Cheng and G.-X. Xu, "A Phase Diagram of the Alloys of the Dysprosium-Copper Binary System," *Acta Phys. Sinica, 31*(6), 807-809 (1982) in Chinese. (Equi Diagram, Crys Structure; Experimental)

82Fra: E. Franceschi, "On the Dy-Cu System," *J. Less-Common Met., 87,* 249-256 (1982). (Equi Diagram, Crys Structure; Experimental)

82Gra: H. de Graaf, R.C. Thiel, and K.H.J. Buschow, "Magnetic Properties and ^{155}Gd Mossbauer Effect in $GdCu_2$ and its Ternary Hydride," *J. Phys. F, 12,* 1239-1245 (1982). (Crys Structure; Experimental)

***83Car:** M.M. Carnasciali, S. Cirafici, and E. Franceschi, "On the Gd-Cu System," *J. Less-Common Met., 92,* 143-147 (1983). (Equi Diagram, Crys Structure; Experimental; #)

83Cha: M.W. Chase, "Heats of Transition of the Elements," *Bull. Alloy Phase Diagrams, 4*(1), 123-124 (1983). (Thermo; Compilation)

83Che: C.S. Cheng and L.-M. Zeng, "A Phase Diagram of the Alloys of the Gd-Cu Binary System," *Acta Phys. Sinica, 32*(11), 1443-1448 (1983) in Chinese. (Equi Diagram, Crys Structure; Experimental; #)

83Don: J.C.M. van Dongen, T.T.M. Palstra, A.F.J. Morgownik, J.A. Mydosh, B.M. Geerken, and K.H.J. Buschow, "Crystal-Structure Transformations and Magnetic-Ordering Phenomena in $GdCu_{1-x}Ga_x$," *Phys. Rev. B, 27*(3), 1887-1902 (1983). (Crys Structure; Experimental)

83Nie: A.K. Niessen, F.R. de Boer, R. Boom, P.F. de Chatel, W.C.M. Mattens, and A.R. Miedema, "Model Predictions for the Enthalpy of Formation of Transition Metal Alloys II," *Calphad, 7*(1), 51-70 (1983). (Thermo; Theory)

85Gsc: K.A. Gschneidner, Jr., private communication (1985). (Equi Diagram; Review)

86Gsc: K.A. Gschneidner, Jr. and F.W. Calderwood, "Intra Rare Earth Binary Alloys: Phase Relationships, Lattice Parameters and Systematics," in *Handbook on the Physics and Chemistry of Rare Earths,* Vol. 8, K.A. Gschneidner, Jr. and L. Eyring, Ed., North-Holland Physics Publishing Co., Amsterdam, 1-161 (1986). (Equi Diagram, Crys Structure; Compilation)

*Indicates key paper.

#Indicates presence of a phase diagram.

Cu-Gd evaluation contributed by **P.R. Subramanian,** Materials Science Division, Universal Energy Systems, Incorporated, 4401 Dayton-Xenia-Road, Dayton, OH 45435 and **D.E. Laughlin,** Department of Metallurgical Engineering and Materials Science, Carnegie Mellon University, Pittsburgh, PA 15213. Work was supported by ASM INTERNATIONAL and the Department of Energy through the Joint Program on Critical Compilation of Physical and Chemical Data coordinated through the Office of Standard Reference Data, National Bureau of Standards. The authors wish to thank Dr. K.A. Gschneidner, Jr., Director, and F.W. Calderwood, Rare-earth Information Center, Ames Laboratory, Iowa State University, Ames, IA, for providing part of the bibliographic search and the computer program for the critical evaluation of crystallographic data. The authors would also like to thank Dr. D.J. Chakrabarti, ALCOA, for his assistance with some of the computer programs, and Mr. Pei Shiyou (Carnegie Mellon University) for providing the English translation of [83Che]. Literature searched through 1985. Professor Laughlin is the ASM/NBS Data Program Category Editor for binary copper alloys.

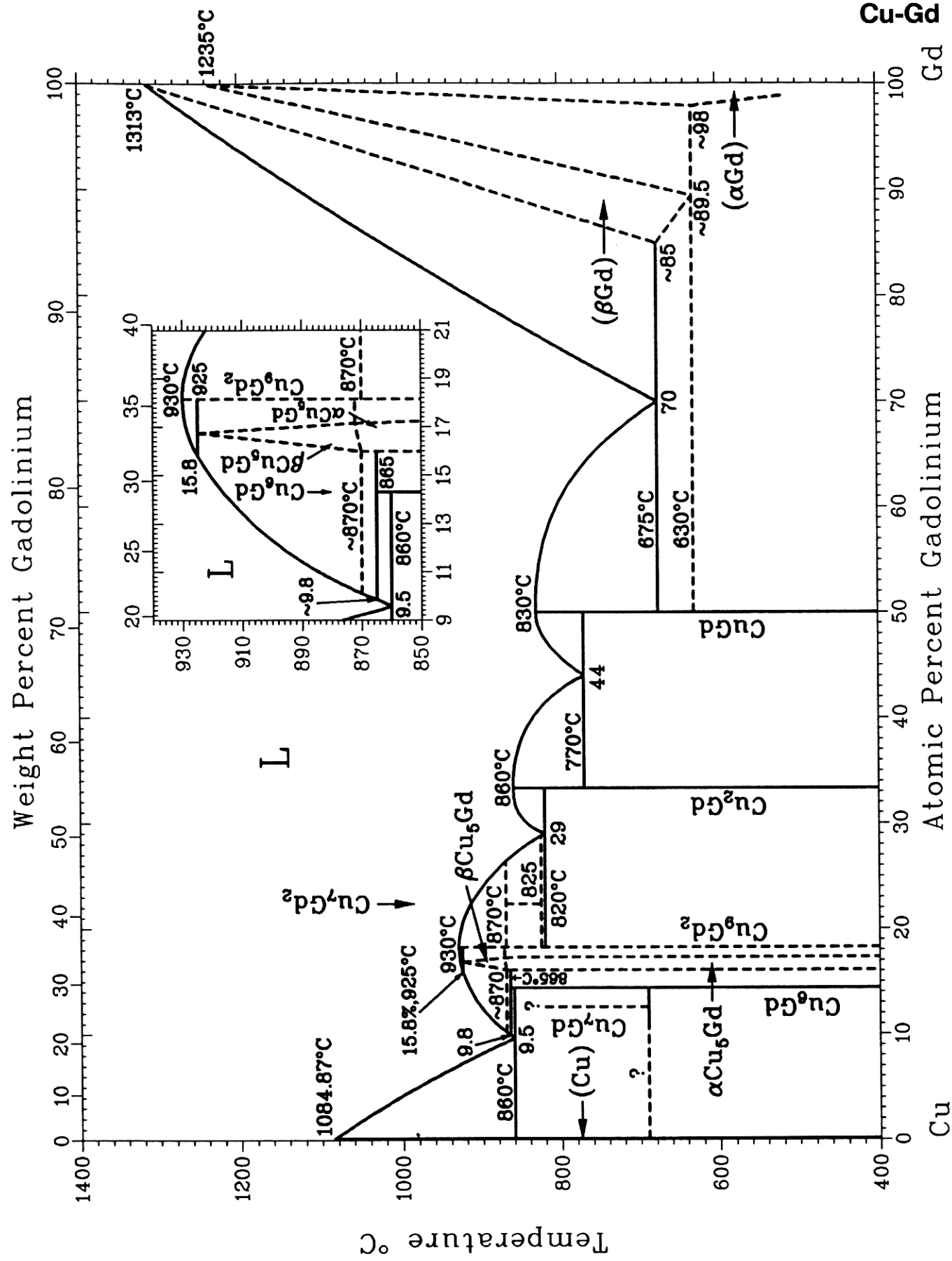

P.R. Subramanian and D.E. Laughlin

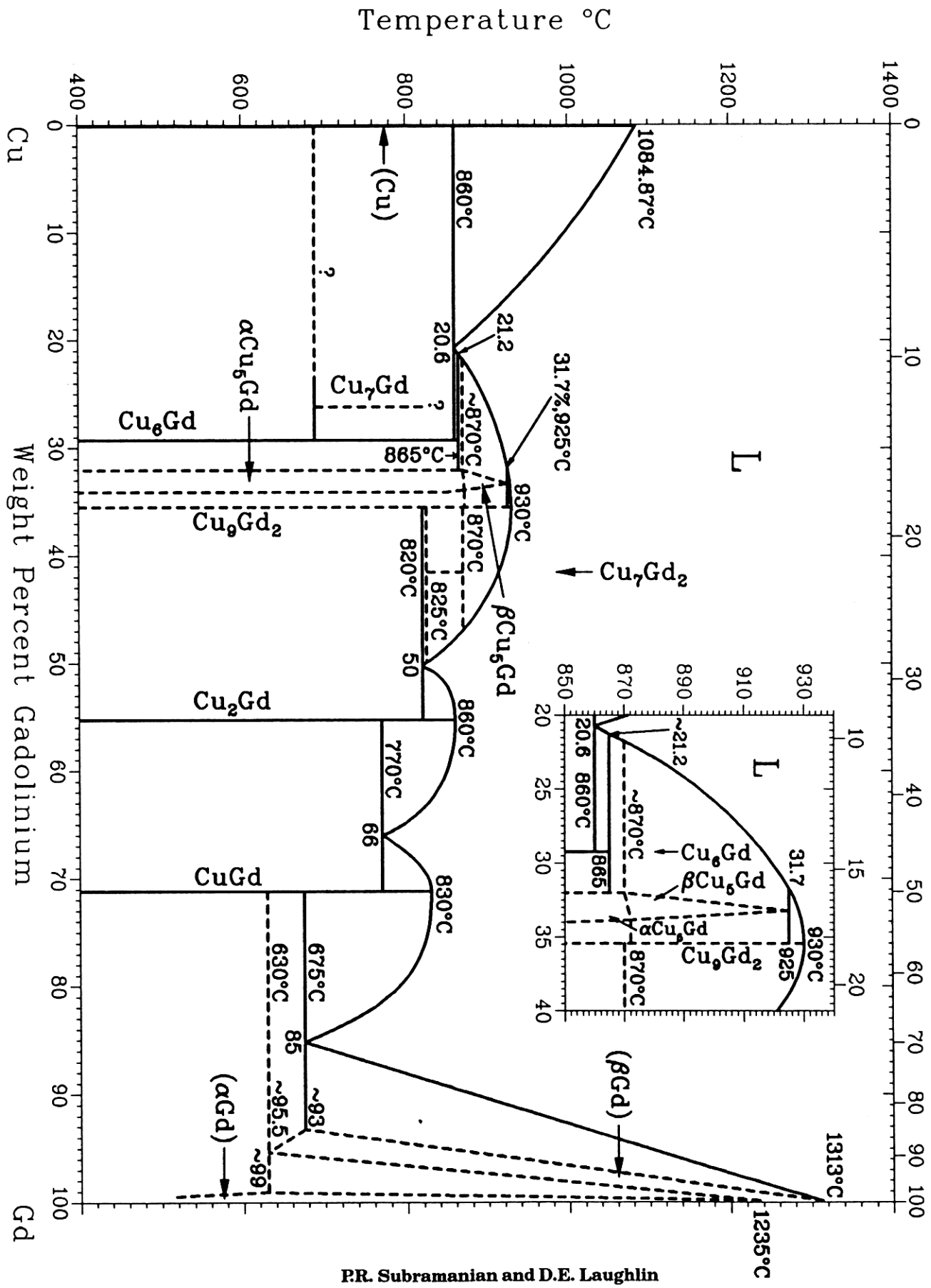

P.R. Subramanian and D.E. Laughlin